WALAILAK JOURNAL
http://wjst.wu.ac.th Health Sciences

Cholinesterase Inhibitory Activity, Kinetic and Molecular Docking Studies of *N*-(1-substituted-1*H*-1,2,3-triazole-4-yl)-aralkylamide Derivatives

Woralak PETRAT[1], Chatchai WATTANAPIROMSAKUL[2], Teerapat NUALNOI[3], Nadia Hanim SABRI[4], Vannajan Sanghiran LEE[4] and Luelak LOMLIM[1,*]

[1]*Department of Pharmaceutical Chemistry, Faculty of Pharmaceutical Sciences, Prince of Songkla University, Songkhla 90112, Thailand*
[2]*Department of Pharmacognosy and Pharmaceutical Botany, Faculty of Pharmaceutical Sciences, Prince of Songkla University, Songkhla 90112, Thailand*
[3]*Department of Pharmaceutical Technology, Faculty of Pharmaceutical Sciences, Prince of Songkla University, Songkhla 90112, Thailand*
[4]*Department of Chemistry, Faculty of Science, University of Malaya, Kuala Lumpur 50603, Malaysia*

([*]Corresponding author's e-mail: luelak.l@psu.ac.th)

Received: 16 February 2016, Revised: 27 August 2016, Accepted: 23 September 2016

Abstract

Acetylcholinesterase (AChE) inhibitors are widely used for treatment of Alzheimer's disease (AD). With the ultimate goal of improving the efficiency of AChE inhibitors currently used in AD treatment, in this study, a total number of 14 compounds of *N*-(1-substituted-1*H*-1,2,3-triazole-4-yl)-aralkylamide derivatives were designed, synthesized, and investigated for their AChE and butyrylcholinesterase (BuChE) inhibitory activities. The most potent AChE inhibitor in this series was **6e** (IC_{50} 15.01 μM against human AChE). The inhibition kinetics of **6e** indicated that the compound was a noncompetitive inhibitor of acetylcholinesterase. A molecular docking study supported the idea that the aromatic moieties of **6e** interacted with both a catalytic anionic site and a peripheral anionic site of acetylcholinesterase, while the 1,2,3-triazole ring also formed van der Waals and hydrogen bond interactions with the amino acid residues in the mid-gorge of the enzyme.

Keywords: 1,2,3-triazole, acetylcholinesterase inhibitor, butyrylcholinesterase inhibitor, enzyme kinetic study, molecular docking

Introduction

Alzheimer's disease (AD) is a degenerative neurologic disorder that causes irreversible loss of neurons and intellectual abilities. Acetylcholine (ACh) and the associated neurons play important roles in cognition, learning and memory. A decrease in ACh levels leads to impairment of these functions and has been considered to be one of the major causes of AD. In addition, many factors, such as beta-amyloid aggregation, oxidative stress, and abnormal phosphorylation of tau protein, are also considered to be involved in AD pathogenesis [1].

Acetylcholinesterase (AChE) is an ACh-degrading serine protease mainly found at the cholinergic synapses. Inhibition of AChE results in an increased cholinergic function that in turn provides therapeutic benefit towards AD. Butyrylcholinesterase (BuChE) is another cholinesterase found in the human body. While AChE is abundant in the brain, muscles and erythrocyte membrane, BuChE has a higher activity in the liver, intestine, heart, lungs and plasma. In AD patients, AChE activity decreases to three-fourths,

compared to the normal brain, while BuChE activity increases. The change in the ratio of AChE to BuChE as the disease progresses indicates that BuChE may also have a role in regulating ACh [2,3]. Structurally, the active site of AChE is a deep and narrow gorge containing a catalytic anionic site (CAS) at the bottom and a peripheral anionic site (PAS) at the entrance [4]. Tacrine, galantamine and donepezil are AChE inhibitors (AChEIs) commonly used for AD treatment, **Figure 1**. However, the AChE inhibitions by these drugs are mechanistically different. While tacrine and galantamine mainly bind to the CAS, donepezil acts as a dual binding site inhibitor, as it has affinities for both CAS and PAS sites. Many dual binding site inhibitors have shown a higher affinity to AChE than inhibitors that bind only to CAS. Additionally, these compounds can interfere with AChE-mediated beta-amyloid aggregation, which is believed to be another cause of AD. Therefore, compounds of this class would have additional benefits, since they act on multiple targets involved in the pathophysiology of AD [5,6].

Aromatic stacking interactions with the CAS are essential for AChE inhibition, as demonstrated by many AChE inhibitors. In addition, many aromatic amino acids are found in the PAS and are responsible for the binding of inhibitor molecules. Many dual binding site inhibitors share structural features as 2 aromatic moieties connected with a linker of suitable length, allowing them to bind to both anionic sites simultaneously.

1,2,3-triazole is a scaffold widely used for the development of various biological active compounds, such as dopamine D_3 receptor [7], antimalarial [8], anticancer and antimicrobial [9], and nicotinic receptor ligands [10], etc. In the design and synthesis of acetylcholinesterase inhibitors, the scaffold has been used as a linker connecting 2 aromatic moieties in many molecules. For example, in *anti*-triazole regioisomer, derived from tacrine and phenylphenanthridinium azides, *anti*1TZ2PA6 (**Figure 1**), the triazole ring had van der Waals contacts with the tyrosine (Tyr-341) side chain of acetylcholinesterase from *Torpedo californica* (*Tc*AChE), and N2 and N3 of the triazole ring developed hydrogen bonds with Tyr-337 in the mid-gorge region of AChE [11]. In a series of more potent inhibitors of AChE, triazole-containing berberine derivatives (**Figure 1**), molecular modeling revealed that the triazole ring displayed a face-to-face π-π stacking interaction with tryptophan (Trp-84) and phenylalanine (Phe-330) in the CAS region [12]. Due to the involvement of 1,2,3-triazole moiety in binding interactions between inhibitors and the active site of AChE, this scaffold has been actively utilized in the design of many AChEIs recently reported in literature, such as 9*H*-carbazole derivatives [13], acridone linked to 1,2,3-triazole derivatives [14], 4-hydroxycoumarin derivatives containing substituted benzyl-1,2,3-triazole moiety [15], acridone-1,2,4-oxadiazole-1,2,3-triazole hybrids [16], and 1,2,3-triazole derivatives with morpholinoethanamine side chains [17].

In 2012, our group reported on the design and synthesis of some *N*-(1-substituted-1*H*-1,2,3-triazole-4-yl)-aralkylamides (**6a** - **6f**) as AChEIs. Both aromatic moieties were expected to interact with both the CAS and the PAS, and the 1,2,3-triazole linker may be responsible for interaction with the mid-gorge of AChE. Preliminary results indicated that compounds in this series were promising AChE inhibitors [18]. This prompted us to synthesize more *N*-(1-substituted-*1H*-1,2,3-triazole-4yl)-aralkyl-amide derivatives (**6g** - **6n**) in order to explore the structure-activity relationships (SARs). In addition, AChE and BuChE inhibitory activity in all synthesized compounds was investigated, and the mode of enzyme inhibition was defined. Finally, a molecular docking study was employed to provide insights into the interactions between the investigated compounds and the AChE enzyme.

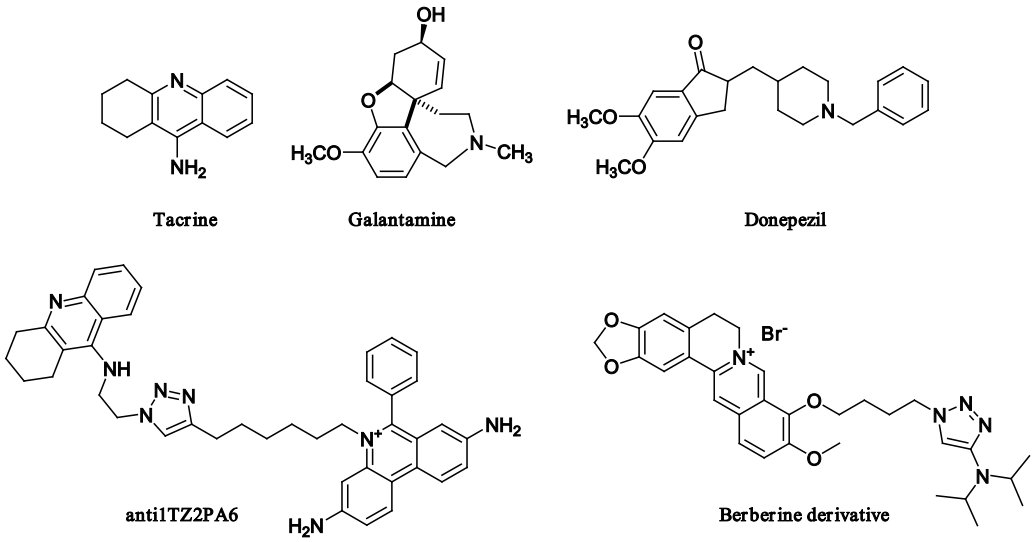

Figure 1 Structure of some AChEIs

Materials and methods

Thin-layer chromatography was carried out using silica gel G 60 F_{254} aluminium sheets. Column chromatography was performed with silica gel. Melting points (mp) were determined using Mel-TempII melting point apparatus. Fourier transform infrared (FTIR) spectra were obtained from a Perkin-Elmer Spectrum One Infrared Spectrophotometer. ^{1}H- and ^{13}C- Nuclear magnetic resonance (NMR) spectra were recorded on a Varian UNITY INOVA Nuclear Magnetic Resonance Spectrometer (500 and 125 MHz for ^{1}H- and ^{13}C-NMR, respectively). Mass spectra were recorded on a Thermo Finnegan MAT 95 XL Mass Spectrometer. Ellman's assay was performed using a Biotex Power Wave$_x$ Microplate Reader. All materials were purchased from common commercial suppliers and used without further purification.

Synthesis of *N*-(1-substituted-1*H*-1,2,3-triazole-4-yl)-aralkylamide derivatives

Compounds **6a** - **6f**, as well as their intermediates (**2a** - **2c**, **5a** - **5b**), were synthesized and characterized in our previous work [18]. This article reports on the synthesis and characterization of compounds **2d**, **5c** - **5d** and **6g** - **6n** using the same method, as shown in **Figure 2**.

Synthesis of (2-azidoethyl) benzene (2d)

(2-Chloroethyl) benzene (**1d**) (1 mol) was dissolved in 10 mL of dimethyl sulfoxide in a round-bottomed flask equipped with a stirrer; sodium azide (2 mol) was then added into the flask and the reaction mixture was stirred overnight. The reaction mixture was quenched using ice-water and extracted with diethyl ether, washed successively with 5 % sodium bicarbonate solution, and dried over anhydrous sodium sulphate. The solvent was removed by rotary evaporation. The product was purified by column chromatography to obtain (2-azidoethyl) benzene (**2d**).

General method for the synthesis of propargyl amides (5c - 5d)

Corresponding benzoic acid derivatives (**3c** - **3d**) (1 mol) were dissolved in 10 ml of dimethyl formamide in a round-bottomed flask. Then, 1-ethyl-3-(3-dimethylaminopropyl) carbodiimide (EDCI, 1 mol), 4-dimethylaminopyridine (DMAP, 0.5 mol), and propargyl amine (1 mol) were added. The reaction mixture was stirred overnight under nitrogen gas, and the progress of the reaction was monitored by thin-layer chromatography. After the reaction was completed, the reaction mixture was extracted with ethyl

acetate, washed with saturated sodium chloride solution, and dried over anhydrous sodium sulphate. The solvent was removed by rotary evaporation. The products were purified by column chromatography and recrystallized by ethyl acetate and hexane to give the propargyl amide derivatives.

General method for the synthesis of triazole compounds (6g - 6n)

Benzyl azide derivative (**2a** - **2c**) or (2-azidoethyl) benzene (**2d**) (1 mol) and propargyl amide derivative (**5a** - **5d**) (1 mol) were mixed in a round-bottomed flask and dissolved in ethanol. 0.1 M Copper sulfate solution (0.2 mL) and copper powder (16 mg) were added. The reaction mixture was stirred at room temperature under nitrogen gas for 2 - 4 days. The reaction mixture was filtered and the solvent was removed by rotary evaporation. The residue was extracted with ethyl acetate, washed with water and saturated sodium chloride solution, and dried under sodium sulphate anhydrous. The solvent was removed using a rotary evaporator. The products were purified by column chromatography and recrystallized by ethyl acetate and hexane.

***In vitro* inhibition study on AChE and BuChE**

The assay for cholinesterase inhibitory activity was modified from the method of Ellman [19]. Rivastigmine and donepezil were used as positive controls. Concentration of the inhibitor equaled 100 μM. The assay was carried out by adding 125 μL of 3 mM 5,5′-dithiobis(2-nitrobenzoic acid) (DTNB), 25 μL of 1.5 mM acetylthiocholine iodide (ACTI), 50 μL of 50 mM Tris-HCl buffer pH 8.0, and 25 μL of sample dissolved in ethanol to the 96-well plate, followed by adding 25 μL of AChE enzyme. The velocities of the reactions were measured by reading the absorbance at 405 nm every 11 sec for 2 min using a microplate reader. Inhibitory activity was calculated using the following equation: % inhibition = [(Mean velocity of blank - Mean velocity of sample)/Mean velocity of blank] × 100. The half maximal inhibitory concentration (IC_{50}) determination was performed with 8 concentrations of samples (100 - 0.78 μM) using AChE from *Electrophorus electricus* and AChE from human erythrocytes. The data was analyzed using the Graph-Pad Prism 4.03 software for IC_{50} values. Each sample was analyzed in triplicate.

BuChE inhibitory activity was evaluated in the same manner using the BuChE enzyme from horse serum. 1.5 mM Butyrylthiocholine iodide was used as a substrate. Determination of the IC_{50} was performed with 7 concentrations of samples (100 - 0.78 μM) using BuChE from horse serum and human BuChE. IC_{50} values were calculated using the Graph-Pad Prism software.

Assay of inhibition kinetics

Compound **6e** was selected for the kinetic study using AChE from *Electrophorus electricus*. The velocities of the reaction in the presence and absence of the inhibitor were measured by the spectrophotometric method, as described above. Three concentrations of the inhibitor, 8, 16, and 32 μL, were chosen for the assay. For each concentration of the inhibitor, the concentration of the substrate ACTI was varied from 50 to 16,000 μM. The result was displayed in a Lineweaver-Burk plot, in which the reciprocal of initial velocity (1/v) was plotted against the reciprocal of substrate concentration (1/[S]). The mode of inhibition of compound **6e** was evaluated by a global non-linear regression fit using the kinetic inhibition analysis mode of the Graph-Pad Prism software.

Molecular docking studies

In order to obtain the initial structures, 2 ligands Donepezil and **6e** were optimized using density functional theory (DFT) at the B3LYP/6-311G level. It was carried out using the Gaussian 09 package programme [20]. Optimized geometry was used in the docking process. The pdb file of the target protein (PDB ID: 1EVE), with a resolution of 2.5 Å, was obtained from the Research Collaboratory for Structural Bioinformatics (RCSB) protein data bank (http://www.pdb.org). The docking procedure was conducted by using the CDOCKER protocol for receptor-ligand interactions of the Discovery Studio Client 2.5. The CHARMm force field and MMFF94 partial charge were applied [21]. Basically, translating the center of the ligand to a specified position within the active site of the protein will produce a series of random

rotations. Thus, random orientations of the conformation are generated. Each orientation was made accountable to simulate the annealing molecular dynamics that involve heating up to a high temperature and cooling down to a target temperature. In order to ensure the ligand binding was well within the target protein, the site sphere was selected according to the binding location of the donepezil. The docking calculations were performed inside a sphere with a radius of 15 Å. Fifty poses were sorted for each ligand based on the CHARMm energy, and a complex structure was selected based on the CDOCKER interaction energy.

The binding energy was calculated by using the calculated binding energies protocol. This allowed us to estimate the binding energy between the target protein and the ligand. In order to get the binding energy, the 10 best poses of each ligand were used. Those complex structures with low interaction energy of CDOCKER were further minimized in the same manner and analyzed in detail. The interaction energy of the ligands with AChE within 3 Å was further explored by the interaction energy protocol.

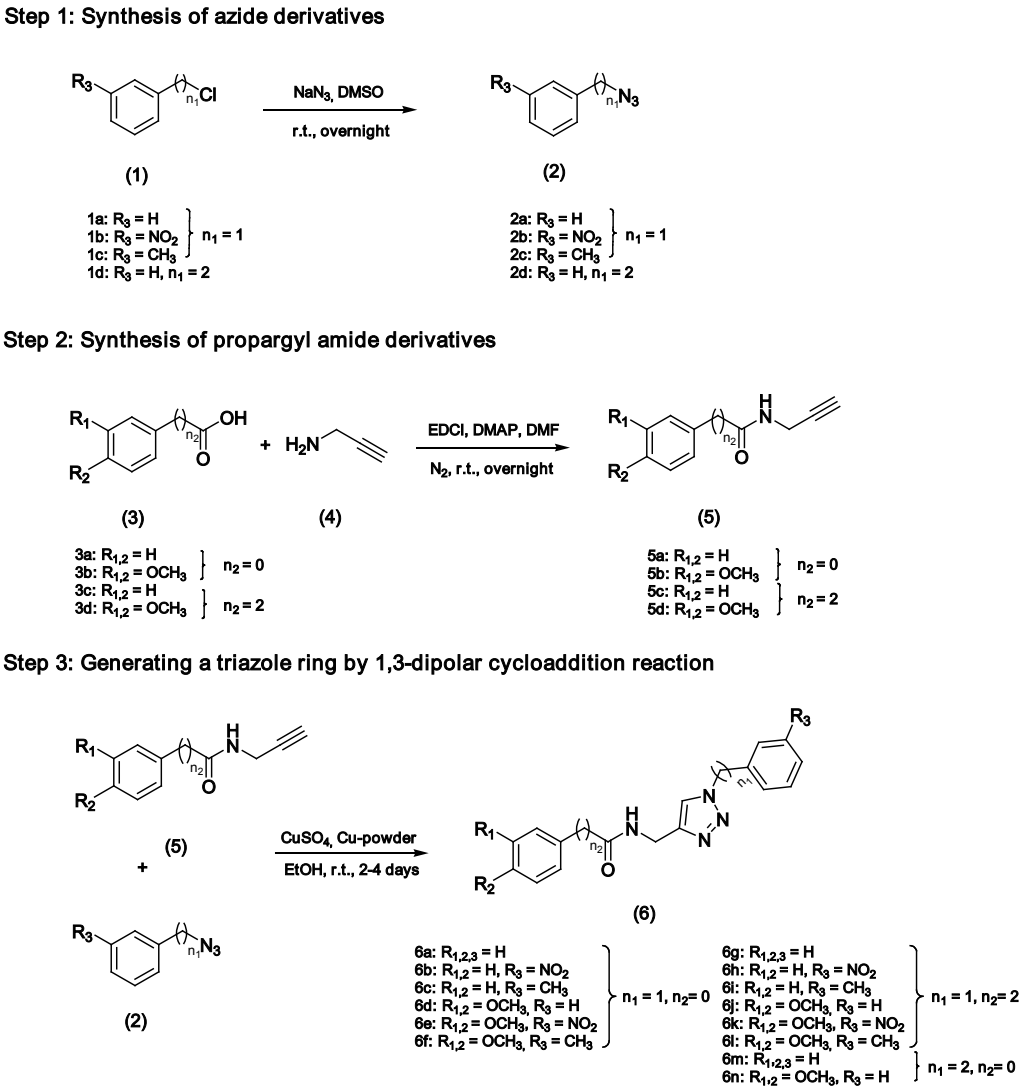

Figure 2 Synthesis of *N*-(1-substituted-1*H*-1,2,3-triazole-4-yl)-aralkylamide derivatives (**6a** - **6n**).

Results and discussion

Chemistry

Synthesis and characterization of compound **6a** - **6f** were reported in our previous study [18]. Compounds **6g** - **6n** and their intermediates were obtained in high yields. Chemical structures of the final products (**6g** - **6n**) were elucidated by ^{1}H-NMR, ^{13}C-NMR, mass spectrometry, and high-resolution mass spectrometry, and were found to correspond with the proposed structures. Characterization details of the synthesized compounds are as follows;

(2-azidoethyl) benzene (2d)

Hexane:dichloromethane (80:20) was used as mobile phase for column chromatography. 75 % yield. colorless liquid. FTIR (neat, cm^{-1}): 3404, 2930, 2098, 1257; ^{1}H-NMR (500 MHz, DMSO-d_6): δ (ppm) 2.84 (2H, *t*, *J* = 7.0, -CH_2-N_3), 3.54 (2H, *t*, *J* = 7.0, -CH_2-), 7.20-7.31(5H, *m*, aromatic H).

3-Phenyl-*N*-(prop-2-ynyl) propanamide (5c)

Dichloromethane:ethtylacetate (80:20) was used as mobile phase for column chromatography. 84 % yield. white solid. mp 70 - 72 °C. FTIR (KBr, cm^{-1}): 3275, 3062, 1634, 1546, 301, 1011; ^{1}H-NMR (500 MHz, DMSO-d_6): δ (ppm) 2.38 (2H, *t*, *J* = 8.2, -CH_2-), 2.80 (2H, *t*, *J* = 7.55, -CH_2-), 3.06 (1H, *t*, *J* = 2.52, -CH- in alkyne), 3.84 (2H, *dd*, *J* = 2.97, *J* = 2.52, -CH_2-), 7.25-7.28 (5H, *m*, aromatic H), 8.25 (1H, *t*, *J* = 5.50, -NH-).

3-(3,4-Dimethoxyphenyl)-*N*-(prop-2-ynyl)propanamide (5d)

Dichloromethane:ethtylacetate (80:20) was used as mobile phase for column chromatography. 75 % yield. White solid. mp 127-129°C. FTIR (KBr, cm^{-1}): 3263, 3057, 1638, 1518, 1255, 1156; ^{1}H-NMR (500 MHz, DMSO-d_6): δ (ppm) 2.34 (2H, *t*, *J* = 8.05, -CH_2-), 2.73 (2H, *t*, *J* = 8.05, -CH_2-), 3.06 (1H, *t*, *J* = 2.44, -CH- in alkyne), 3.69 (3H, *s*, -OCH_3), 3.71 (3H, *s*, -OCH_3-), 3.83 (2H, *dd*, *J* = 2.92, *J* = 2.69, -CH_2-), 6.68 (1H, *,d*, *J* = 6.10, *J* = 1.95, aromatic H), 6.78 (1H, *d*, *J* = 1.95, aromatic H), 6.82 (1H, *d*, *J* = 8.29, aromatic H), 8.25 (1H, *t*, *J* = 5.50, -NH-).

***N*-((1-Benzyl-1H-1,2,3-triazol-4-yl)methyl)-3-phenylpropanamide (6g)**

Dichloromethane:ethtylacetate (50:50) was used as mobile phase for column chromatography. 77 % yield. White solid. mp 125-127 °C. FTIR (KBr, cm^{-1}): 3304, 3070, 1638, 1548, 1221, 1029; ^{1}H-NMR (500 MHz, DMSO-d_6): δ (ppm) 2.38 (2H, *t*, *J* = 8.03, -CH_2-), 2.80 (2H, *t*, *J* = 8.03, -CH_2-), 4.27 (2H, *d*, *J* = 5.44, -CH_2-), 5.55 (2H, *s*,-CH_2-), 7.15-7.25 (5H, *m*, aromatic H), 7.30-7.40 (5H, *m*, aromatic H), 7.80 (1H, *s*, -CH-N-), 8.30 (1H, *t*, *J* = 5.44, -NH-); ^{13}C-NMR (125 MHz, DMSO-d_6): δ (ppm) 31.12 (-CH_2-), 34.29 (-CH_2-), 36.91 (-CH_2-), 52.85 (-CH_2-), 122.90 (-CH-N-), 125.98, 128.07, 128.24, 128.33, 128.36, 128.86 (aromatic C), 136.23 (-<u>C</u>-CH_2-), 141.40 (-<u>C</u>-CH_2CH_2-), 145.42 (=C-N-), 171.36 (-C=O) ; EI-MS *m/z*: 90.9 (100 %), 319.7 (59 %), 186.8 (12 %), 104.9 (11 %), 320.7 (11 %), 76.9 (4 %); HR-MS m/z: 320.1632 (Calcd for $C_{19}H_{20}N_4O$: 320.1632).

***N*-((1-(3-Nitrobenzyl)-1H-1,2,3-triazol-4-yl)methyl)-3-phenylpropanamide (6h)**

Dichloromethane:ethtylacetate (80:20) was used as mobile phase for column chromatography. 81 % yield. White solid. mp 121-123 °C. FTIR (KBr, cm^{-1}): 3289, 3083, 1644, 1557, 1353, 1524, 1237; ^{1}H-NMR (500 MHz, DMSO-d_6): δ (ppm) 2.39 (2H, *t*, *J* = 7.50, -CH_2-), 2.79 (2H, *t*, *J* = 7.50, -CH_2-), 4.27 (2H, *d*, *J* = 6.00, -CH_2), 5.72 (2H, *s*, -CH_2-), 7.10-7.25 (5H, *m*, aromatic H), 7.69 (1H, t, *J* = 7.00, aromatic H), 7.75 (1H, *d*, *J* = 7.50, aromatic H), 7.90 (1H, *s*, -CH-N-), 8.18 (1H, *d*, *J* = 1.00, aromatic H), 8.21 (1H, s, aromatic H), 8.31 (1H, t, *J* = 5.50, -NH-) ; ^{13}C-NMR (125 MHz, DMSO-d_6): δ (ppm) 31.12 (-CH_2-), 34.27 (-CH_2-), 36.93 (-CH_2-), 51.79 (-CH_2-), 123.28 (-CH-N-), 122.90, 123.25, 125.96, 128.33, 128.35, 130.54, 134.84 (aromatic C), 138.36 (-<u>C</u>-CH_2-), 141.40 (-<u>C</u>-CH_2CH_2-), 145.61 (=C-N-), 148.03 (-C-NO_2), 171.40 (-C=O); EI-MS *m/z*: 90.9 (100 %), 364.6 (97 %), 135.8 (68 %), 104.9 (40 %), 231.7 (31 %), 365.6 (21 %); HR-MS m/z: 365.1482 (Calcd for $C_{19}H_{19}N_5O_3$: 365.1482).

***N*-((1-(3-Methylbenzyl)-1H-1,2,3-triazol-4-yl)methyl)-3-phenylpropanamide (6i)**

Hexane:eththylacetate (20:80) was used as mobile phase for column chromatography. 78 % yield. White solid. mp 101-123 °C. FTIR (KBr, cm^{-1}): 3376, 3065, 1651, 1520, 1217; ^{1}H-NMR (500 MHz, DMSO-d_6): δ (ppm) 2.28 (3H, *s*, -CH_3-), 2.38 (2H, *t*, *J* = 7.50, -CH_2-), 2.80 (2H, *t*, *J* = 7.50, -CH_2-), 4.26 (2H, *d*, *J* = 5.50, -CH_2-), 5.49 (2H, *s*, -CH_2-), 7.08 (1H, *d*, *J* = 7.00, aromatic H), 7.12 (1H, *d*, *J* = 1.50, aromatic H), 7.15 (1H, *t*, *J* = 7.00, aromatic H), 7.17 (1H, *s*, aromatic H), 7.19-7.27 (5H, *m*, aromatic H), 7.75 (1H, *s*, -CH-N-), 8.28 (1H, *t*, *J* = 5.50, -NH-) ; ^{13}C-NMR (125 MHz, DMSO-d_6):δ (ppm) 21.05 (-CH_3), 31.13 (-CH_2-), 34.29 (-CH_2-), 36.92 (-CH_2-), 52.87 (-CH_2-), 122.85 (-CH-N-), 125.23, 125.98, 128.33, 128.35, 128.68, 128.77, 128.88 (aromatic C), 136.11 (-C-CH_2-), 138.08 (-C-CH_3), 141.40 (-C-CH_2CH_2-), 145.39 (=C-N-), 171.36 (-C=O) ; EI-MS *m/z*: 104.9 (100 %), 333.7 (68 %), 334.7 (14 %), 90.9 (24 %), 200.8 (15 %), 105.9 (7 %); HR-MS m/z: 334.1788 (Calcd for $C_{20}H_{22}N_4O$: 334.1788).

***N*-((1-Benzyl-1H-1,2,3-triazol-4-yl)methyl)-3-(3,4-dimethoxyphenyl)propanamide (6j)**

Hexane:eththylacetate (20:80) was used as mobile phase for column chromatography. 72 % yield. White solid. mp 117-119 °C. FTIR (KBr, cm^{-1}): 3365, 2950, 1646, 1520, 1262, 1025; ^{1}H-NMR (500 MHz, DMSO-d_6): δ (ppm) 2.36 (2H, *t*, *J* = 7.50, -CH_2-), 2.73 (2H, *t*, *J* = 7.50, -CH_2-), 3.70 (6H, *s*, -OCH_3), 4.26 (2H, *d*, *J* = 5.50, -CH_2-), 5.55 (2H, *s*,-CH_2-), 6.66 (1H, *dd*, *J* = 6.00, *J* = 2.00, aromatic H), 6.77 (1H, *d*, *J* = 2.00, aromatic H), 6.79 (1H, *d*, *J* = 8.50, aromatic H), 7.28-7.38 (5H, *m*, aromatic H), 7.80 (1H, *s*, -CH-N), 8.98 (1H, *t*, *J* = 5.50, -NH-); ^{13}C-NMR (125 MHz, DMSO-d_6): δ (ppm) 30.77 (-CH_2-), 34.29 (-CH_2-), 37.23 (-CH_2-), 52.85 (-CH_2-), 55.51 (-OCH_3), 55.70 (OCH_3), 112.06, 112.38, 120.09, 128.07, 128.24, 128.86 (aromatic C), 122.93 (-CH-N-), 133.93 (-C-CH_2-), 136.23 (-C-CH_2CH_2-), 145.42 (=C-N-), 147.20 (-C-OCH_3), 148.74(-C-OCH_3), 171.51(-C=O); EI-MS (m/z): 379.6 (100 %), 90.9 (91 %), 163.9 (84 %), 150.9 (57 %), 186.8 (12 %), 192.8 (4 %), 380.6(21 %); HR-MS (M+) : 380.1843 (calcd. For $C_{21}H_{24}N_4O_3$: 380.1843).

3-(3,4-Dimethoxyphenyl)-*N*-((1-(3-nitrobenzyl)-1H-1,2,3-triazol-4-yl) methyl)propanamide (6k)

Hexane:eththylacetate (20:80) was used as mobile phase for column chromatography. 78 % yield. White solid. mp 143-145 °C. FTIR (KBr, cm^{-1}): 3283, 2948, 1648, 1563, 1520, 1352, 1352, 1026; ^{1}H-NMR (500 MHz, DMSO-d_6): δ (ppm) 2.36 (2H, *t*, *J* = 7.50, -CH_2-), 2.73 (2H, *t*, *J* = 7.50, -CH_2-), 3.70 (6H, *s*, -OCH_3), 4.27 (2H, *d*, *J* = 6.00, -CH_2-), 5.70 (2H, *s*, -CH_2-), 6.66 (1H, *dd*, *J* = 6.00, *J* = 2.00, aromatic H), 6.77 (1H, *d*, *J* = 2.00, aromatic H), 6.80 (1H, *t*, *J* = 8.00, aromatic H), 7.69 (1H, *t*, *J* = 7.00, aromatic H), 7.74 (1H, *d*, *J* = 7.00, aromatic H), 7.95 (1H, *s*, -CH-N-), 8.18 (1H, *d*, *J* = 1.00, aromatic H), 8.21 (1H, *s*, aromatic H), 8.98 (1H, *t*, *J* = 5.50, -NH-); ^{13}C-NMR (125 MHz, DMSO-d_6): δ (ppm) 30.78 (-CH_2-), 34.27 (-CH_2-), 37.26 (-CH_2-), 51.78 (-CH_2-), 55.51 (-OCH_3), 55.70 (-OCH_3), 122.88(-CH-N-), 112.08, 112.37, 120.08, 123.24, 123.32, 130.53, 138.36 (aromatic C), 133.92(-C-CH_2-), 134.82(-C-CH_2CH_2-), 145.61 (=C-N-), 147.20 (-C-OCH_3), 148.03 (-C-NO_2), 148.74 (-C-OCH_3), 171.54 (-C=O) ; EI-MS *m/z*: 163.8 (100 %), 150.9 (77 %), 135.6 (21 %), 424.5 (66 %), 425.5 (12 %), 231.7 (5 %); HR-MS m/z: 425.1694 (Calcd for $C_{21}H_{23}N_5O_5$: 425.1694).

3-(3,4-Dimethoxyphenyl)-*N*-((1-(3-methylbenzyl)-1H-1,2,3-triazol-4-yl) methyl)propanamide (6l)

Eththylacetate was used as mobile phase for column chromatography. 88 % yield. White solid. mp 60-62 °C. FTIR (KBr, cm^{-1}): 3373, 2942, 1648, 1518, 1231, 1028; ^{1}H-NMR (500 MHz, DMSO-d_6): δ (ppm) 2.28 (3H, *s*, -CH_3), 2.36 (2H, *t*, *J* = 7.50, -CH_2-), 2.74 (2H, *t*, *J* = 7.50, -CH_2-), 3.70 (6H, *s*, -OCH_3), 4.23 (2H, *d*, *J* = 5.50, -CH_2-), 5.44 (2H, *s*, -CH_2-), 6.66 (1H, *dd*, *J* = 6.00, *J* = 2.00, aromatic H), 6.77 (1H, *d*, *J* = 2.00, aromatic H), 6.80 (1H, *t*, *J* = 8.00, aromatic H), 7.08(1H, *d*, *J* = 8.50, aromatic H), 7.12 (1H, *s*, aromatic H), 7.13 (1H, *d*, *J*= 9.00, aromatic H), 7.24(1H, *t*, *J* = 8.00, aromatic H), 7.80 (1H, *s*, -CH-N-), 8.25 (1H, *t*, *J* = 5.50, -NH-); ^{13}C-NMR (125 MHz, DMSO-d_6): δ (ppm) 21.05 (-CH_3), 30.79 (-CH_2-), 34.29 (-CH_2-), 37.25 (-CH_2-), 52.86 (-CH_2-), 55.52 (-OCH_3), 55.70 (-OCH_3), 122.89 (-CH-N-), 112.07, 112.38, 120.10, 125.21, 128.67, 128.78, 128.88 (aromatic C), 133.93 (-C-CH_2-), 136.11 (-C-CH_2CH_2-), 138.09 (-C-CH_3), 145.40 (=C-N-), 147.21 (-C-OCH_3), 148.75 (-C-OCH_3), 171.52 (-C=O); EI-MS *m/z*:

393.6 (100 %), 104.9 (65 %), 163.8 (60 %), 150.9 (58 %), 394.6 (23 %), 90.9 (11 %), 200.8 (10 %); HR-MS m/z: 394.1999 (Calcd for $C_{22}H_{26}N_4O_3$: 394.1999).

***N*-((1-phenethyl-1H-1,2,3-triazol-4-yl)methyl)benzamide (6m)**

Dichloromethane:methanol (90:10) was used as mobile phase for column chromatography. 94 % yield. White solid. mp 115-117 °C. FTIR (KBr, cm^{-1}): 3387, 3064, 1641, 1520, 1290; ^{1}H-NMR (500 MHz, DMSO-d_6): δ (ppm) 3.12 (2H, *t*, *J* = 7.6, -CH_2-), 4.47 (2H, *d*, *J* = 5.6, -CH_2-NH), 4.55 (2H, *t*, *J* = 7.6, -CH2-), 7.18-7.25 (5H, *m*, aromatic H), 7.43-7.54 (3H, *m*, aromatic H), 7.86 (2H, *t*, *J* = 5.9, aromatic H), 7.88 (1H, *s*, -CH-N-), 8.97 (1H, *t*, *J* = 5.6, -NH-) ; ^{13}C-NMR (125 MHz, DMSO-d_6): δ (ppm) 34.75 (-CH_2-), 35.79 (-CH_2-NH), 50.46 (-CH_2-), 126.52 (-CH-N-), 134.35 (-C-CH_2-), 123.01, 127.37, 128.38, 128.51, 128.80, 131.26, 137.68 (aromatic C), 145.13 (=C-N-), 165.99 (C=O); EI-MS *m/z*: 104.9 (100 %), 305.8 (89 %), 186.9 (66 %), 200.9 (33 %), 77.0 (22 %), 306.8 (18 %), 91.0 (8 %); HR-MS m/z: 306.1475 (Calcd for $C_{18}H_{18}N_4O$: 306.1475).

3,4-dimethoxy-*N*-((1-phenethyl-1H-1,2,3-triazol-4-yl)methyl)benzamide (6n)

Dichloromethane:methanol (90:10) was used as mobile phase for column chromatography. 93 % yield. White solid. mp 122 - 124 °C. FTIR (cm^{-1}): 3327, 3121, 2931, 1633, 1508, 1229, 1021; ^{1}H-NMR (500 MHz, DMSO-d_6): δ (ppm) 3.12 (2H, *t*, *J* = 7.5, -CH2-), 3.78 (6H, 2*s*, -OCH_3), 4.44 (2H, *d*, *J* = 6.0, -CH_2-NH), 4.55 (2H, *t*, *J* = 7.5, -CH_2-), 6.99 (1H, *d*, *J* = 8.3, aromatic H), 7.17-7.26 (5H, *m*, aromatic H), 7.45 (1H, *d*, *J* = 2.0, aromatic H), 7.48-7.50 (1H, *dd*, *J* = 8.3, 2.0, aromatic H), 7.84 (1H, *s*, -CH-N-), 8.84 (1H, *t*, *J* = 5.5, -NH-); ^{13}C-NMR (125 MHz, DMSO-d_6): δ (ppm) 34.74 (-CH_2-), 35.59 (-CH_2-NH), 50.27 (-CH_2-), 55.69 (-OCH_3), 55.73 (-OCH_3), 120.59 (-CH-N-), 110.83, 111.02, 122.81, 126.55, 126.62, 128.47, 128.78, 137.69 (aromatic C), 145.05 (=C-N-), 148.18 (-C-OCH_3), 151.26 (-C-OCH_3), 165.53 (-C=O); EI-MS *m/z*: 164.9 (100 %), 365.8 (78 %), 200.9 (38 %), 366.8 (19 %), 105.0 (27 %), 77.0 (15 %), 91.0 (13 %), 136.9 (9 %); HR-MS m/z: 366.1686 (Calcd for $C_{20}H_{22}N_4O_3$: 366.1686).

***In vitro* inhibition study on AChE and BuChE**

In the screening test, electric eel AChE was used due to it being commercially available and highly similar (89 % similarity) to human AChE, with 100 % amino acid identity in the catalytic triad (https://blast.ncbi.nlm.nih.gov). All synthesized 1,2,3-triazole compounds exhibited both AChE and BuChE inhibitory activities. At the concentration of 100 μM, the compounds inhibited AChE and BuChE in a range of about 40 - 69 % and 26 - 51 %, respectively (**Table 1**).

Among derivatives **6a** - **6f** (n_1 = 1, n_2 = 0), we found that replacing the R_1 and R_2 groups with OCH_3 provided compounds with a higher AChE inhibitory activity than those without substituents on the benzamide moiety. Previous research showed that the OCH_3 substituents on the indanone moiety of donepezil formed van der Waals forces with amino acid residues at the PAS of the enzyme [22]. Thus, it was possible that OCH_3 substituents in compounds **6d** - **6f** were responsible for a higher inhibitory activity through van der Waals interactions with the target, as demonstrated in the previous study. The effect of replacing the R_3 position with electron withdrawing or electron donating groups on % inhibition was not clearly observed. Structural modifications on the R_1, R_2 and R_3 positions affected the BuChE inhibitory activity in the same way as in the AChE inhibitory activity. However, the BuChE inhibitory activity of compound **6b** was higher than the BuChE inhibitory activity of compound **6e**, while the AChE inhibitory activity of compound **6b** was lower than the AChE inhibitory activity of compound **6e**.

Since the length of the alkyl chain linking the aromatic moieties and the 1,2,3-triazole ring system could affect the distance between both aromatic centers and the flexibility of the molecule, in this study, we also varied the length of the linker at position n_1 and n_2. Elongation of the linker connecting the 1,2,3-triazole ring and the aromatic moiety in compounds **6g** - **6i** (n_1 = 1, n_2 = 2) led to a slight increase in its AChE inhibitory activity when compared to the corresponding derivatives **6a** - **6c** (n_1 = 1, n_2 = 0). In contrast, compounds **6j** - **6l** (n_1 = 1, n_2 = 2), with OCH_3 groups on R_1 and R_2 positions, exhibited a lower activity than their counterparts, **6d** - **6f** (n_1 = 1, n_2 = 0). Nevertheless, lengthening of the linker tended to result in a decreased BuChE inhibitory activity among the compounds in this series. Replacing the N1 of

triazole ring with a phenylethyl group in compounds **6m** and **6n** resulted in a comparable and decreased cholinesterase activity compared to its counterpart (**6a** and **6d**), respectively.

The length of the alkyl chain linking the aromatic moieties and the 1,2,3-triazole ring system affected the distance between both aromatic centers, as well as the flexibility of the molecule, and resulted in a different binding affinity. In this study, we found that the shorter linker (n_1 = 1, n_2 = 0) provided a more suitable distance between the aromatic centers and restricted rotation of the alkyl chain so that the aromatic rings could fit into the enzyme binding pocket and exert inhibitory activity.

Compounds **6d** - **6f**, the top 3 AChE inhibitors from the series, were further evaluated for their cholinesterase inhibitory activities, using rivastigmine and donepezil as reference compounds (**Table 2**). Compounds **6d** - **6f** displayed higher potency in electric eel AChE inhibitory activity than rivastigmine, with an IC_{50} in the range of 4.90 - 8.30 μM. The compound with the highest potency in this series was **6e** (IC_{50} 4.90±0.66 μM). This result indicated that replacing the R_3 position with the electron-withdrawing nitro group gave higher potency in AChE inhibition. Compounds **6d** - **6f** showed a lower potency to BuChE from horse serum (IC_{50} 43.31 - 79.66 μM) compared to electric eel AChE. In contrast to the AChE inhibitory activity, electron-withdrawing substituent at the R_3 position (in compound **6e**) decreased BuChE inhibitory activity. Substitution of R_3 with the methyl group gave the most potent BuChE inhibitor in this series (compound **6f**, IC_{50} 43.31±2.93 μM).

Compounds **6d** - **6f** exhibited moderate inhibitory activity against human AChE (IC_{50} 15.01 - 59.20 μM), but low inhibitory activity against human BuChE. (IC_{50} >100 μM) Compound **6e** was still the most potent acetylcholinesterase inhibitor in this series (IC_{50} 15.01 ± 0.14 μM).

Table 1 Cholinesterase inhibitory activity of 1,2,3-triazole derivatives.

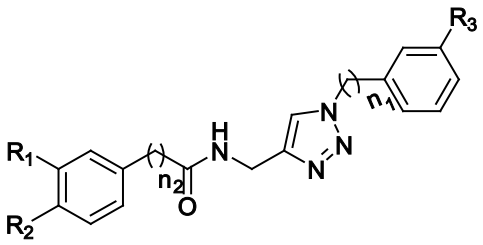

Compound	n_1	n_2	R_1	R_2	R_3	% Inhibition (100 μM)	
						AChE[a]	BuChE[b]
6a	1	0	H	H	H	41.68	35.63
6b	1	0	H	H	NO_2	46.70	51.00
6c	1	0	H	H	CH_3	42.24	33.32
6d	1	0	OCH_3	OCH_3	H	60.75	48.29
6e	1	0	OCH_3	OCH_3	NO_2	65.80	43.50
6f	1	0	OCH_3	OCH_3	CH_3	68.68	44.44
6g	1	2	H	H	H	43.36	32.47
6h	1	2	H	H	NO_2	49.10	41.27
6i	1	2	H	H	CH_3	45.15	42.58
6j	1	2	OCH_3	OCH_3	H	45.79	45.27
6k	1	2	OCH_3	OCH_3	NO_2	46.87	30.67
6l	1	2	OCH_3	OCH_3	CH_3	39.83	26.29
6m	2	0	H	H	H	41.52	38.83
6n	2	0	OCH_3	OCH_3	H	53.66	37.45
Rivastigmine						61.37	60.23
Donepezil						99.79	93.71

[a]AChE enzyme from electric eel (n = 3), [b]BuChE enzyme from horse serum (n = 3).

Table 2 IC_{50} for cholinesterase inhibitory activity of compounds **6d - 6f**.

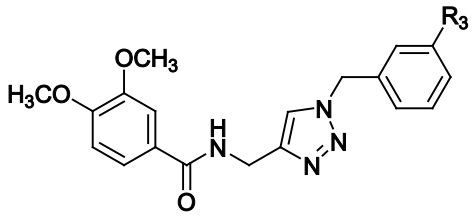

Compound	R_3	IC_{50} (μM±SEM)			
		AChE[a]	BuChE[b]	AChE[c]	BuChE[d]
6d	H	8.25 ± 0.26	58.13 ± 1.49	47.61 ± 1.58	> 100
6e	NO_2	4.90 ± 0.66	79.66 ± 1.30	15.01 ± 0.14	> 100
6f	CH_3	8.30 ± 0.53	43.31 ± 2.93	59.20 ± 0.91	> 100
Rivastigmine	-	26.97 ± 1.36	45.65 ± 0.64	1.31 ± 0.07	12.26 ± 0.94
Donepezil	-	0.022 ± 0.001	1.64 ± 0.19	0.0014 ± 0.0004	1.11 ± 0.06

[a]AChE enzyme from electric eel (n = 3), [b]BuChE enzyme from horse serum (n = 3), [c]AChE enzyme from human erythrocytes (n = 3), [d]BuChE, human, recombinant expressed in transgenic goats (n = 3)

Kinetic analysis of AChE inhibition

The inhibition kinetics of compound **6e** were investigated using the modified Ellman's method and presented by overlaid Lineweaver-Burk plots (**Figure 3**). The plots showed that the K_m values of the substrate were unchanged when the inhibitor concentration was increased, indicating that compound **6e**, and presumably the other compounds in this series, were noncompetitive inhibitors. The result suggested that the compounds might inhibit AChE through an allosteric mechanism. It has been proposed that binding of an inhibitor with the peripheral site of the enzyme prompts a movement of the Ω loop and allosterically alters the orientation of Trp-84 in the CAS [23]. The analysis also revealed that compound **6e** had a K_i value of 27.87 μM.

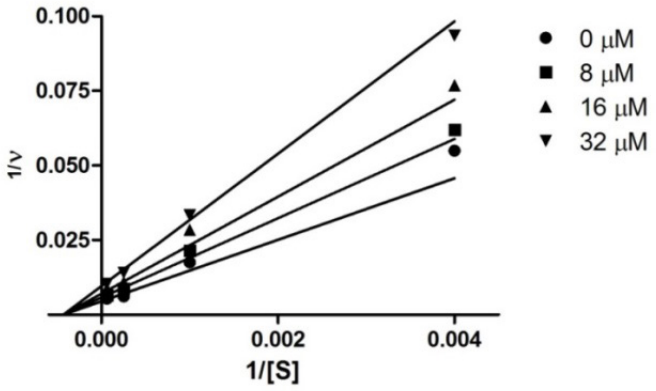

Figure 3 Lineweaver-Burk plot for inhibition of AChE by compound **6e**.

Molecular docking study

Optimization of the geometry of each ligand was performed when their geometry was adjusted until a stationary point on the potential surface was reached. Based on the results, the geometry for optimization of the energy values for the ligand (donepezil and **6e**) were -1212.73 Ha and -1385.55 Ha, respectively. The binding sites of 1EVE were Trp84, Asp72, Tyr121, Ser200, Trp279, Phe290, Phe330, Phe331, Tyr 334, and His440 [24]. **Table 3** shows the results of the molecular docking of 1EVE with different ligands.

Superposition of the docking structures is shown in **Figure 4**. According to the docking results, donepezil has slightly more-CDOCKER interaction energy, which indicated a better activity than **6e**, due to the substituent in **6e** that increased the steric effect. The IC_{50} (μM) illustrated the inhibitory abilities of the compound, and this value correlated with the interaction energy. According to **Figure 5(A)**, donepezil had a hydrogen bond formed with 1EVE at the Tyr121 residue, which is represented as a green dashed line. There is a pi-pi stacking interaction between the benzylpiperidine moiety of donepezil and the indole ring of Trp84 of the catalytic anionic site, which is represented by the yellow dashed line in **Figure 5**. At the PAS site, the indanone moiety of donepezil interacted with the indolic group of Trp279 via a classical parallel pi-pi interaction, as indicated by the blue dashed line in **Figure 5(A)**. In **Figure 5(B)**, the 3-nitrobenzyl moiety of compound **6e** exhibited a pi-pi interaction with Trp 84. The triazole ring was also shown to form van der Waals and hydrogen bond interactions with the amino acid residues in the mid-gorge of the AChE, which enhanced the binding affinity to AChE. At the PAS site, a pi-pi interaction was also observed between the substituted benzamide moiety and Trp 279.

The details of the total interaction energy of the van der Waals (VDW) and electrostatic forces with amino acids within 3 Å of the AChE of the minimized complex structures from the CDOCKER protocol are tabulated in **Table 4**. Donepezil indicated a stronger binding interaction when compared to **6e**. Donepezil was found to exhibit some interaction with both Phe 330 and Trp84, whilst **6e** interacted with Tyr334. Both of the stated interactions come from a strong van der Waals interaction.

The interactions observed from molecular docking supported our hypothesis that the aromatic moieties interact with the aromatic side chains of the amino acid residues in both the CAS and PAS sites, and the triazole ring also plays a role in the binding of the amino acid residues in the mid-gorge of the AChE. The compounds in this series are not as potent as *anti*1TZ2PA6, which is composed of strong CAS and PAS ligands connected by the 1,2,3-triazole linker. The *N*-(1-substituted-1*H*-1,2,3-triazole-4-yl)-aralkylamide compounds in this series can be used as lead compounds for further optimization for the development of acetylcholinesterase inhibitors.

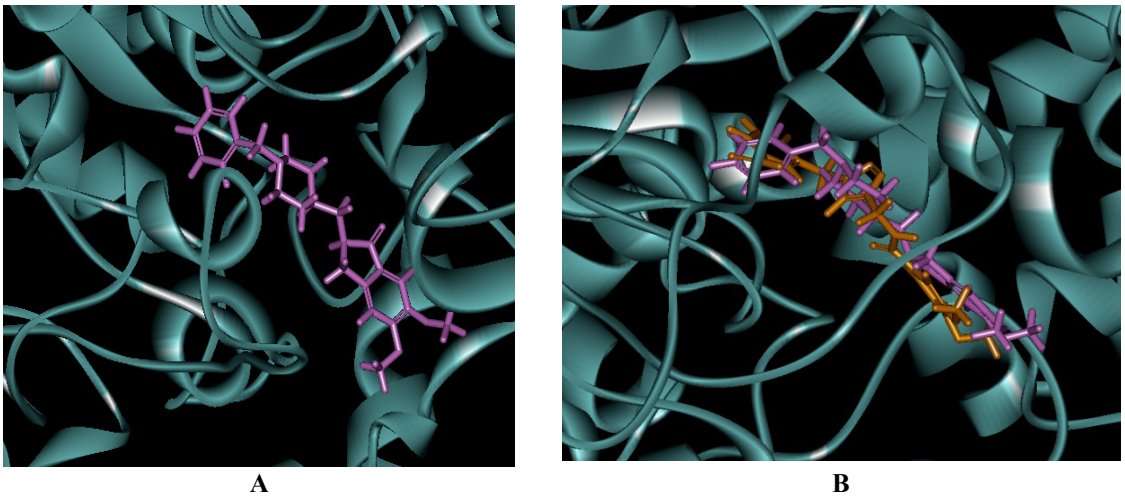

A **B**

Figure 4 (A) Docking of donepezil to 1EVE, (B) superimposed donepezil (purple), and **6e** (yellow).

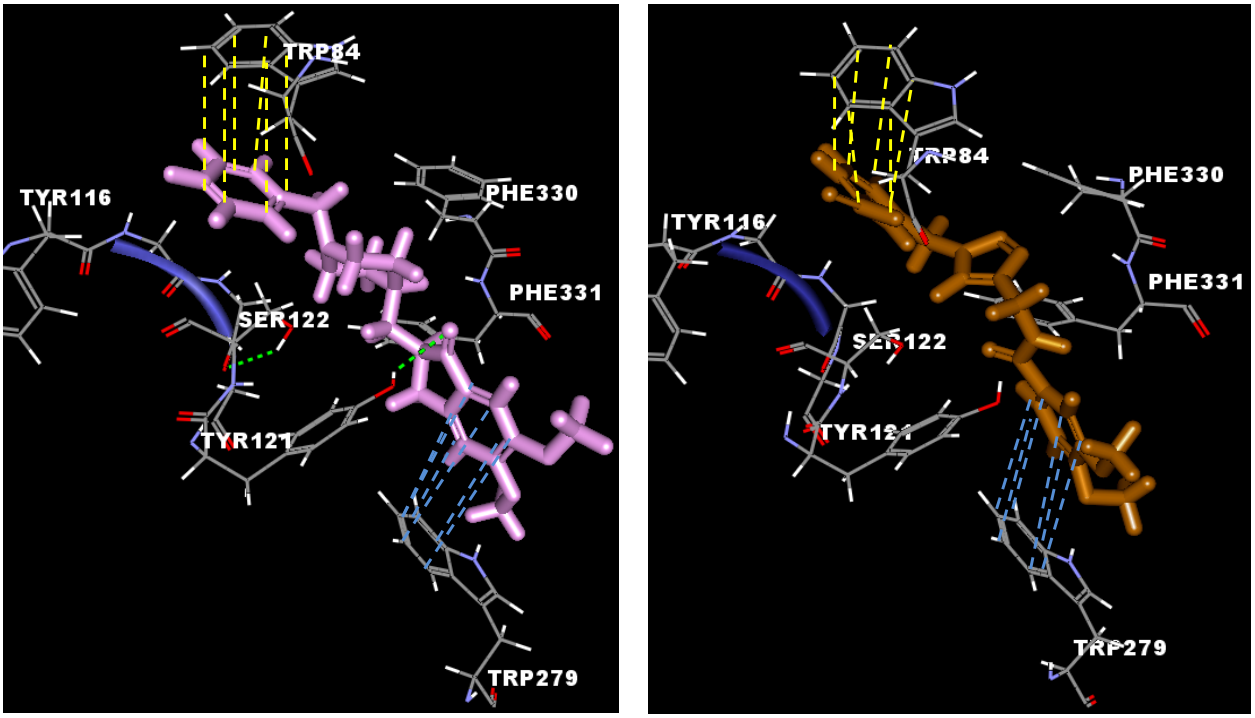

Figure 5 The docking conformation and the AChE amino acid interactions with (A) donepezil and (B) **6e**.

Table 3 Results of molecular docking of ligands with AChE. Energy is in kcal/mol.

Ligand	$IC_{50} \pm SEM^a$ (μM)	-CDOCKER interaction energy	Binding energy
Donepezil	0.022	45.57	–51.62
6e	4.90	45.37	–49.72

[a]AChE enzyme from electric eel (n = 3)

Table 4 Contribution of interaction energy in kcal/mol of protein from binding residues within 3Å. as highlighted in bold letters.

Residue	Interaction Energy (IE)	VDW	Electrostatic	Residue	Interaction Energy (IE)	VDW	Electrostatic
Donepezil				**6e**			
A_TYR70	**-8.22335**	**-2.20915**	**-6.0142**	**A_TYR70**	**-1.28896**	**-1.85927**	**0.570308**
A_TRP84	**-9.38289**	**-3.73743**	**-5.64546**	**A_TRP84**	**-2.85074**	**-1.50955**	**-1.34119**
A_GLY117	**-2.79708**	**-1.71602**	**-1.08106**	**A_GLY117**	**-2.39481**	**-1.79011**	**-0.6047**
A_GLY118	**-2.23564**	**-2.37034**	**0.1347**	**A_GLY118**	**-5.55373**	**-2.51039**	**-3.04334**
A_TYR121	**-4.76819**	**-2.81225**	**-1.95594**	**A_TYR121**	**-4.46447**	**-1.90905**	**-2.55542**
A_SER122	**-0.47681**	**-2.17127**	**1.69446**	**A_SER122**	**-0.28399**	**-1.78314**	**1.49915**
A_TYR130	**-0.173435**	**-0.583774**	**0.410339**	A_TYR130	-3.53487	-0.629727	-2.90514
A_GLU199	1.52875	-0.723697	2.25245	**A_GLU199**	**3.31146**	**0.406208**	**2.90525**
A_TRP279	**-2.32896**	**-3.83656**	**1.5076**	A_TRP279	-0.95337	-3.9807	3.02733
A_ILE287	**-1.90597**	**-0.929515**	**-0.976453**	A_ILE287	-1.2795	-0.600175	-0.679326
A_PHE290	**-3.41463**	**-2.27284**	**-1.14179**	**A_PHE290**	**-2.88727**	**-1.88703**	**-1.00024**
A_PHE330	**-10.9516**	**-3.98549**	**-6.96612**	**A_PHE330**	**-4.97307**	**-1.89051**	**-3.08256**
A_PHE331	**1.64213**	**-1.70405**	**3.34618**	**A_PHE331**	**-2.16976**	**-3.22682**	**1.05706**
A_TYR334	**-3.05979**	**-3.72324**	**0.663448**	**A_TYR334**	**-6.08625**	**-3.67384**	**-2.41241**
A_GLY335	**-1.75734**	**-0.659306**	**-1.09803**	A_GLY335	5.25956	-0.193411	5.45297
A_HIS440	-7.50802	-1.51433	-5.99369	**A_HIS440**	**-4.15019**	**-2.02579**	**-2.1244**
A_GLY441	**-0.875745**	**-0.9117**	**0.035955**	**A_GLY441**	**0.551478**	**0.048436**	**0.503042**
A_ILE444	**-0.413609**	**-0.75329**	**0.339681**	**A_ILE444**	**-4.72058**	**-1.17891**	**-3.54167**
Total surface IE within 3 Å	-51.12291	-34.37622	-16.74669	Total surface IE within 3 Å	-37.96089	-24.78977	-13.17112
Total IE	-57.10219	-36.61425	-20.48793	Total IE	-38.46908	-30.19379	-8.2753

Conclusions

N-(1-substituted-1*H*-1,2,3-triazole-4-yl)-aralkylamide derivatives have been demonstrated to be moderately potent cholinesterase inhibitors. The most potent compound, **6e**, was a noncompetitive acetylcholinesterase inhibitor, with an IC_{50} value of 15.01 ± 0.14 μM against human AChE. Molecular docking revealed that compound **6e** acted as a dual binding site AChE inhibitor. These compounds can be used as lead compounds for the further development of acetylcholinesterase inhibitors.

Acknowledgements

This research was financially supported by Prince of Songkla University (Project Number PHA550299S) and the University of Malaya for computer and software facilities.

References

[1] A Lleó, SM Greengerg and JH Growdon. Current pharmacotherapy for Alzheimer's disease. *Annu. Rev. Med.* 2006; **57**, 513-33.
[2] NH Greig, T Utsuki, QS Yu, X Zhu, HW Holloway, TA Perry, B Lee, DK Ingram and DK Laniri. A new therapeutic target in Alzheimer's disease treatment: attention to butyrylcholinesterase. *Curr. Med. Res. Opin.* 2001; **17**, 159-65.
[3] GA Reid, N Chilukuri and S Darvesh. Butyrylcholinesterase and the cholinergic system. *Neuroscience* 2013; **234**, 53-68.
[4] JL Sussman, M Harel, F Frolow, and G Oefner, A Goldman, L Toker and I Silman. Atomic structure of acetylcholinesterase from *Torpedo californica*: A prototypic acetylcholine-binding protein. *Science* 1991; **253**, 872-8.
[5] D Muñoz-Torrero and P Camps. Dimeric and hybrid anti-alzheimer drug candidates. *Curr. Med. Chem.* 2006; **13**: 399-22.
[6] A Cavalli, ML Bolognesi, A Minarini, M Rosini, V Tumiatti, M Recanatini and C Melchiorre. Multi-target-directed ligands to combat neurodegenerative diseases. *J. Med. Chem.* 2008; **51**, 347-72.
[7] TM Keck, AK Banala, RD Slack, C Burzynski, A Bonifazi, OM Okunola-Bakare, M Moore, JR Deschamps, R Rais, BS Slusher and AH Newman. Using click chemistry toward novel 1,2,3-triazole-linked dopamine D3 receptor ligands. *Bioorg. Med. Chem.* 2015; **23**, 4000-12.
[8] HM Faidallah, SS Panda, JC Serrano, AS Girgis, KA Khan, KA Alamry, T Therathanakorn, MJ Meyers, FM Sverdrup and CS Eickhoff. Synthesis, antimalarial properties and 2D-QSAR studies of novel triazole-quinine conjugates. *Bioorg. Med. Chem.* 2016; **24**, 3527-39.
[9] RR Ruddarraju, AC Murugulla, R Kotla, MCB Tirumalasetty, R Wudayagiri, S Donthabakthuni, R Maroju, K Baburao and LS Parasa. Design, synthesis, anticancer, antimicrobial activities and molecular docking studies of theophylline containing acetylenes and theophylline containing 1,2,3-triazoles with variant nucleoside derivatives. *Eur. J. Med. Chem.* 2016; **123**, 379-96.
[10] A Ouach, F Pin, E Bertrand, J Vercouillie, Z Gulhan, C Mothes, JB Deloye, D Guilloteau, F Suzenet, S Chalon and S Routier. Design of α7 nicotinic acetylcholine receptor ligands using the (het) Aryl-1,2,3-triazole core: Synthesis, *in vitro* evaluation and SAR studies. *Eur. J. Med. Chem.* 2016; **107**, 153-64.
[11] Y Bourne, HC Kolb, Z Radic, KB Sharpless, P Taylor and P Marchot. Freeze-frame inhibitors capture acetylcholinesterase in a unique conformation. *Proc. Natl. Acad. Sci. USA*. 2003; **101**, 1449-54.
[12] A Shi, L Huang, C Lu and X Li. Synthesis, biological evaluation and molecular modeling of novel triazole-containing berberine derivatives as acetylcholinesterase and β-amyloid aggregation inhibitors. *Bioorg. Med. Chem.* 2011; **19**, 2298-305.
[13] H Akrami, BF Mirjalili, M Khoobi, A Moradi, H Nadri, A Emami, A Foroumadi, M Vosooghi and A Shafiee. 9*H*-Carbazole derivatives containing the N-benzyl-1,2,3-triazole moiety as new acetylcholinesterase inhibitors. *Arch. Pharm. Chem. Life Sci.* 2015; **348**, 366-74.
[14] M Mohammadi-Khanaposhtani, M Saeedi, NS Zafarghandi, M Mahdavi, R Sabourian, EK Razkenari, H Alinezhad, M Khanavi, A Foroumadi, A Shafiee and T Akbarzadeh. Potent acetylcholinesterase inhibitors: Design, synthesis, biological evaluation, and docking study of acridone linked to 1,2,3-triazole derivatives. *Eur. J. Med. Chem.* 2015; **92**, 799-806.
[15] SM Bagheri, M Khoobi, H Nadri, A Moradi, S Emami, L Jalili-Balen, F Jafarpour, FH Moghadam, A Foroumadi and A Shafiee. Synthesis and anticholinergic activity of 4-hydroxycoumarin derivatives containing substituted benzyl-1,2,3-triazole moiety. *Chem. Biol. Drug. Des.* 2015; **86**, 1215-20.
[16] M Mohammadi-Khanaposhtani, M Mahdavi, M Saeedi, R Sabourian, M Safavi, M Khanavi, A Foroumadi, A Shafiee and T Akbarzadeh. Design, synthesis, biological evaluation, and docking study of acetylcholinesterase inhibitors: New acridone-1,2,4-oxadiazole-1,2,3-triazole hybrids. *Chem. Biol. Drug. Des.* 2015; **86**, 1425-32.

[17] JC Li, J Zhang, MC Rodrigues, DJ Ding, JPF Longo, RC Azevedo, LA Muehlmann and CS Jiang. Synthesis and evaluation of novel 1,2,3-triazole-based acetylcholinesterase inhibitors with neuroprotective activity. *Bioorg. Med. Chem. Lett.* 2016; **26**, 3881-5.
[18] W Petrat, C Wattanapiromsakul and L Lomlim. Design and synthesis of *N*-(1-benzyl-1H-1,2,3-triazole-4-yl)-benzamide derivatives as acetylcholinesterase inhibitor. *In*: Proceedings of the 1st ASEAN Plus Three Graduate Research Congress. Chiang Mai, Thailand, 2012, p. 539-44.
[19] GL Ellman, KD Courtney, V Andres and RM Featherstone. A new and rapid colorimetric determination of acetylcholinesterase activity. *Biochem. Pharmacol.* 1961; **7**, 88-95.
[20] MJ Frisch, GW Trucks, HB Schlegel, GE Scuseria, MA Robb, JR Cheeseman, G Scalmani, V Barone, B Mennucci, GA Petersson, H Nakatsuji, M Caricato, X Li, HP Hratchian, AF Izmaylov, J Bloino, G Zheng, JL Sonnenberg, M Hada, M Ehara, K Toyota, R Fukuda, J Hasegawa, M Ishida, T Nakajima, Y Honda, O Kitao, H Nakai, T Vreven, JA Montgomery, JE Peralta, F Ogliaro, M Bearpark, JJ Heyd, E Brothers, KN Kudin, VN Staroverov, R Kobayashi, J Normand, K Raghavachari, A Rendell, JC Burant, SS Iyengar, J Tomasi, M Cossi, N Rega, JM Millam, M Klene, JE Knox, JB Cross, V Bakken, C Adamo, J Jaramillo, R Gomperts, RE Stratmann, O Yazyev, AJ Austin, R Cammi, C Pomelli, JW Ochterski, RL Martin, K Morokuma, VG Zakrzewski, GA Voth, P Salvador, JJ Dannenberg, S Dapprich, AD Daniels, Ö Farkas, JB Foresman, JV Ortiz, J Cioslowski and DJ Fox. Gaussian 09, Revision C.01. Gaussian, Wallingford CT, 2010.
[21] TA Halgren. Merck molecular force field. I. Basis, form, scope, parameterization, and performance of MMFF94. *J. Comput. Chem.* 1996; **17**, 490-519.
[22] H Sugimoto, H Ogura, Y Arai, Y Iimura and Y Yamanishi. Research and development of donepezil hydrochloride, a new type of acetylcholinesterase inhibitor. *Jpn. J. Pharmacol.* 2002; **89**, 7-20.
[23] S Simon, A Le Goff, Y Frobert, J Grassi and J Massoulie. The binding sites of inhibitory monoclonal antibodies on acetylcholinesterase. *J. Biol. Chem.* 1999; **274**, 27740-6.
[24] F Belluti, L Piazzi, A Bisi, S Gobbi, M Bartolini, A Cavalli, P Valenti and A Rampa. Design, synthesis, and evaluation of benzophenone derivatives as novel acetylcholinesterase inhibitors. *Eur. J. Med. Chem*. 2009; **44**, 1341-8.